Available online at www.sciencedirect.com
SCIENCE DIRECT
Biochimica et Biophysica Acta 1758 (2006) 479–486
BIOCHIMICA ET BIOPHYSICA ACTA
BBA
http://www.elsevier.com/locate/bba

Direct measurement of VDAC–actin interaction by surface plasmon resonance

Inge Roman [a], Jurgen Figys [a,b], Griet Steurs [a,b], Martin Zizi [a,b,*]

[a] *Molecular Membrane Biophysics and Neurophysiology, Dept. of Physiology, Faculty of Medicine and Pharmacy, Vrije Universiteit Brussel, 103 Laarbeeklaan, 1090 Brussels, Belgium*

[b] *Division Studies, Epidemiology and Biostatistics, Department of Defense, 1120 Brussels, Belgium*

Received 31 October 2005; received in revised form 20 February 2006; accepted 16 March 2006
Available online 7 April 2006

Abstract

VDAC – a mitochondrial channel involved in the control of aerobic metabolism and apoptosis – interacts in vitro and in vivo with a wide repertoire of proteins including cytoskeletal elements. A functional interaction between actin and *Neurospora crassa* VDAC was reported, excluding other VDAC isoforms. From a recent genome-wide screen of the VDAC interactome, we found that human actin is a putative ligand of yeast VDAC. Since such interaction may have broader implications for various mitochondrial processes, we probed it with Surface Plasmon Resonance (SPR) technology using purified yeast VDAC (YVDAC) and rabbit muscle G-actin (RGA). We show that RGA binds to immobilized YVDAC in a reversible and dose-dependent manner with saturating kinetics and an apparent K_D of 50 μg/ml (1.2 μM actin). BSA does not bind VDAC regardless of the concentrations. Alternatively, VDAC binds similarly to immobilized RGA but without saturating kinetics. VDAC being known to interact with itself, this latter interaction was directly measured to interpret the RGA signals. VDAC could bind to VDAC without saturating kinetics as expected if higher order binding occurred, and could account for maximally 66% of the non-saturating behavior of VDAC binding onto RGA. Hence, actin–VDAC interactions are not a species-specific oddity and may be a more general phenomenon, the role of which ought to be further investigated.

Keywords: VDAC; Mitochondria; SPR; Actin; Cytoskeleton; Protein–protein interaction

1. Introduction

VDAC is the most abundant protein of the mitochondrial outer membrane or MOM (up to 40% in *Neurospora crassa*). It has an important role in the energy management of the cell by regulating the metabolic fluxes across the mitochondrial membrane [1], and is convincingly involved in the regulation of the apoptotic processes via numerous protein–protein interactions (reviewed in [2,3]). Within the mitochondrial membranes, depending on the isoform, VDAC acts as channel or as an anchoring protein [2]. This protein interacts also with several cytoskeletal elements. Years ago, it has been identified as a binding site for the microtubule-associated protein MAP2 [4]. More recently, its interaction was reported with a component of the cytoplasmic dynein complex that acts as a motor for the intracellular retrograde motility of vesicles and organelles along microtubules [5]. Likewise, functional interactions with gelsolin [6] and with G-actin are also mentioned [7].

As the most abundant proteins in the eukaryotic cell (up to 15% of the total protein content), actin can self-assemble into polymers (F-actin). As part of the cytoskeleton, it has the property to interact with a multitude of actin-binding proteins. Depending on one's definition, there are between 60 and 100 different types of actin-binding proteins (reviewed in [8]). These latter proteins can regulate the assembly of actin, use the actin-based network as scaffold, or contribute to other actin-related functions such as the coordination of elaborate cytoplasmic responses to extra- and intracellular signals. As a

* Corresponding author. Molecular Membrane Biophysics and Neurophysiology, Dept. of Physiology, Faculty of Medicine and Pharmacy, Vrije Universiteit Brussel, 103 Laarbeeklaan, 1090 Brussels, Belgium. Tel.: +32 2 477 4434; fax: +32 2 477 4568.
E-mail address: martin.zizi@vub.ac.be (M. Zizi).

0005-2736/$ - see front matter © 2006 Elsevier B.V. All rights reserved.
doi:10.1016/j.bbamem.2006.03.019

molecular motor, actin is sufficient to drive the rocketing motility of some intracellular bacteria by its polymerisation (reviewed in [9]), and, in mitotic yeast, an actin-dependent mitochondrial motility was identified [10]. In this system, two integral mitochondrial outer membrane proteins – Mmm1p and Mdm10p – together with a peripheral mitochondrial binding protein are needed for the actin–mitochondrion interactions [11]. In the axons of vertebrate neurons, mitochondrial transport occurs along microtubules and F-actin [12]. Regardless of the described model, how mitochondria are attached to the cytoskeleton is still not fully resolved.

It has been shown by Xu et al. that G-actin can modulate the gating of *Neurospora crassa* VDAC [7]. This functional interaction seemed restricted to the NCVDAC isoform. As during a genome-wide scanning of the VDAC interactome, we recently found that the human G-actin is a putative yeast VDAC ligand [13], we tried to directly measure the VDAC–actin interactions using the surface plasmon resonance (SPR) technology.

In this study, the direct and selective binding of G-actin to VDAC is demonstrated. Apparent affinity constants for the VDAC–actin interaction are calculated. Furthermore, direct evidence for VDAC polymerisation is shown, confirming earlier functional reports [14,15].

2. Experimental procedures

2.1. Reagents

All reagents were analytical grade. VDAC from yeast was purified to near homogeneity according to the method of De Pinto et al. [16,17]. G-actin from rabbit muscle and bovine serum albumin (BSA) were purchased from Sigma, Belgium. HBS-EP buffer (0.15 MNaCl, 10 mM HEPES, pH 7.4, 3 mM EDTA, 0.005% polysorbate 20 (v/v), filtered and degassed) and Sensor Chip CM5 were purchased from Biacore, Sweden. NAP™ 10 Columns, Sephadex™ G-25 DNA Grade were purchased from Amersham Pharmacia Biotech AB, Sweden.

2.2. Coupling of Y-VDAC and G-actin to a CM-dextran sensor chip

The VDAC channel was covalently immobilized on a CM5 sensor chip of a Biacore 2000® SPR (Biacore AB, Uppsala, Sweden) by amine coupling, using HBS-N as running buffer. Carboxyl groups on the chip surface were activated by a 10-min injection of a mixture of 100 mM succimide (NHS) and 100 mM carbodiimide (EDC). Different levels of the VDAC protein could be immobilized by varying the injection time (20 or 40 min) or the concentration of VDAC (110 or 66 μg/ml). To avoid that the TRIS buffer interfered with the amine-reactive groups on the chip, purified Y-VDAC was further dissolved in 10 mM K acetate (pH 5.5) supplemented with 1% Triton X-100, and then gel filtered on a NAP™ 10 Column, bringing the protein at a final concentration of 250 μg/ml and a pH lower than the pI of the VDAC protein (pI=8.8). Finally, the un-reacted NH-esters on the chip were deactivated with 1 M ethanolamine pH 8.5 for 10 min. Three different VDAC immobilization levels were used in the experiments [at average binding levels of 2640±160 RU, 5740±300 RU or 10560±540 RU (Resonance Units, mean± S.E.) corresponding to 2.6, 5.7 and 10.6 ng/mm^2, respectively]. After the completion of the immobilization procedure, the chip surface was controlled for stability for a period of 90 min, a maximal baseline drift of 0.08 RU/min was tolerated.

G-actin was coupled using the same amine coupling procedure with an injection of 10 mg/ml G-actin (dissolved in Na Acetate at pH 5.5) for 5 or 10 min. The experiments were performed at three protein immobilization levels of 3690, 1760 and 900 RU [corresponding to 3.7, 1.8 and 0.9 ng/mm^2].

2.3. Surface plasmon resonance analyses

The actin powder was dissolved in milli-Q H_2O as described by the manufacturer yielding a stock solution of 860 μg/ml (20 μM) actin in 0.5 mM Tris, 125 μM mercaptoethanol, 50 μM $CaCl_2$, 50 μM ATP, 1 mM KOH, controlled at pH 12. This solution was further diluted in the experimental running buffer (HBS-EP, see reagents) to 10, 25, 75, 100, 200 and 400 μg/ml actin (controlled final values at pH 7.4–7.7). The binding of G-actin to immobilized YVDAC was measured by SPR in the Biacore2000 device by perfusing in parallel three flow cells having different VDAC immobilization levels, and one flow cell with no VDAC bound as a control. Following one min of stabilized reading with the running buffer only, different actin concentrations were injected during 1.5 min (association phase) at a rate of 30 μl/min, followed by a 15-min dissociation phase. As dilution controls, identical mock solutions (i.e., devoid of VDAC) were also run in the machine before every analyte run (i.e., containing VDAC at the given concentration). Using the BiaEval software, the curves of these mock runs, and of the control flow cell were subtracted from their corresponding analyte binding curves.

The binding of YVDAC to immobilized actin was measured in an analogous manner. YVDAC was dissolved in buffer A (50 mM KCl, 10 mM HEPES, 1 mM EDTA, 1% Triton X-100) after gel filtration, and diluted in the same buffer to 5, 50, 100, 200 m and 500 μg/ml.

For the measurements of YVDAC binding to itself, identical dilutions were prepared. During these experiments the solvent (buffer A) was used as running buffer in the device and the analyte was injected for 3 min. BSA runs against immobilized VDAC were done at 5, 50 and 100 μg BSA/ml, dissolved in buffer A. Binding experiments were performed as described above.

3. Results

3.1. G-actin binds to immobilized YVDAC

Initial binding studies were performed on a chip with a low VDAC-immobilization level around 1000 response units (RU), as recommended for kinetic measurements. In this way the binding rate is determined by the interaction kinetics and not limited by mass transport of the analyte to the surface (Biacore handbook, [18]). In those conditions, a theoretical maximal binding capacity (B_{cap}) can be calculated using the following formula:

$$B_{cap}(\text{in RU}) = n \times \text{captured ligand}(\text{in RU}) \times (\text{MW}_{anal}/\text{MW}_{ligand})$$

In our experiments, VDAC is the captured ligand (MW 30,000) and actin the flowing analyte (MW 43,000). Considering a one to one binding stoichiometry (n), the maximum actin binding response at 1000 RU, would be 1430 RU. As response values were too low at these ligand immobilization levels (less than 1% of predicted values), the dose-dependent interactions between actin and YVDAC were measured at 2200, 5500 and 10000 RU of immobilized bait protein. Fig. 1 (left panel) shows a representative overlay plot of actin binding VDAC at a high immobilization level. Following subtraction of the appropriate control traces (bulk effects of running buffer, sample-dependent mock dilution buffer), the sensorgrams present saturating binding curves. From the plateau values (average of 9 experiments), we could derive the apparent affinity of actin for VDAC (K_D value of 50 μg/ml – equivalent to 1.2 μM – assuming 1-to-1 interaction). At 200 mg/ml – that is at an actin concentration of 4.7 μM – the maximal binding values fell out of the range of

the hyperbolic fit. And, at very high actin concentrations (actin 400 mg/ml) these values became very low (not shown). As the resonance signals depend on the refractive index – thus, the density – near the chip surface and as this decrease of the resonance signal occurs at very high actin concentrations, actin–actin interactions within the sensor chamber could be responsible for such effect.

The specificity of the binding is evidenced by the fact that the binding response of actin was dependent on the immobilization level of VDAC on the chip surface (Fig. 2). The more immobilized VDAC, the more actin binding can be measured. Bovine serum albumin (BSA), a negatively charged protein like actin, was used as negative control. The molecular weight of BSA being of the same order as actin, the magnitudes of the SPR responses if binding occurred should be similar to actin for similar analyte concentrations. As shown in Fig. 3, only actin can bind and no BSA binding occurs as shown by the absence of any measurable SPR signal, even at high BSA concentrations (up to 1.5 μM).

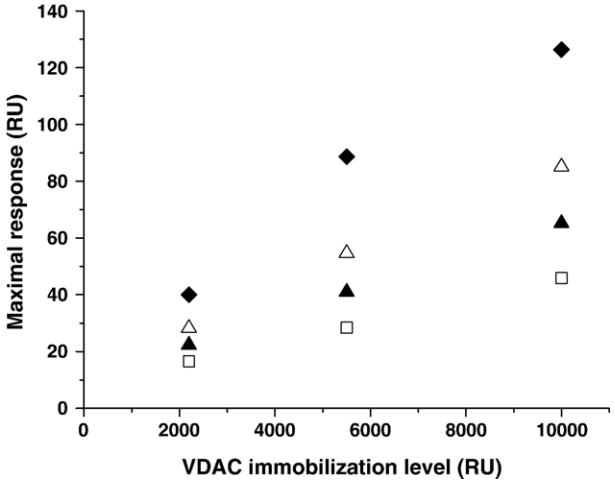

Fig. 2. Maximal binding response of G-actin is proportional to the VDAC immobilization level. The maximal binding values measured for 4 G-actin concentrations 25 (open squares), 75 (triangles), 100 (open triangles) and 200 (diamonds) μg/ml (equals 0.6, 1.7, 2.3 and 4.7 μM) at three different VDAC immobilization levels (2000, 5500 and 10000 RU). The SPR signal increases linearly as expected for selective binding.

3.2. Binding of YVDAC to immobilized G-actin and VDAC–VDAC interactions

Mirroring the previous experiments, actin was used as fixed ligand and VDAC as analyte. Again, more binding is obtained with higher amounts of immobilized molecules as can be seen on the left panel of Fig. 4. This time however the sensorgrams are not simply saturating at high analyte concentrations, as the SPR signal shows a constant slope. This effect is larger at higher actin immobilization levels (see right panel of Fig. 4) with a near 3-fold increase in slope between the lower and higher immobilization levels (see Table 1, lower right column). Hence, no steady state parameters could be derived from the experiments.

As VDAC is known to interact with itself [15,19–21], a VDAC–VDAC binding could cause this continuous increase/drift in SPR signals. Therefore VDAC binding on VDAC was assayed to better interpret these non-saturating data. Fig. 5 presents a dose-dependent binding of VDAC on VDAC itself, and again the concentration-dependent absence of saturation indicates secondary binding during the experiment. The slopes of the sensorgrams of VDAC binding to itself or to actin were compared to assess the contribution of the VDAC–VDAC interactions in the VDAC–actin signal (see Table 1). For VDAC binding to itself, a linear relationship between the slope of the binding (RU divided by time) and the chip immobilization level

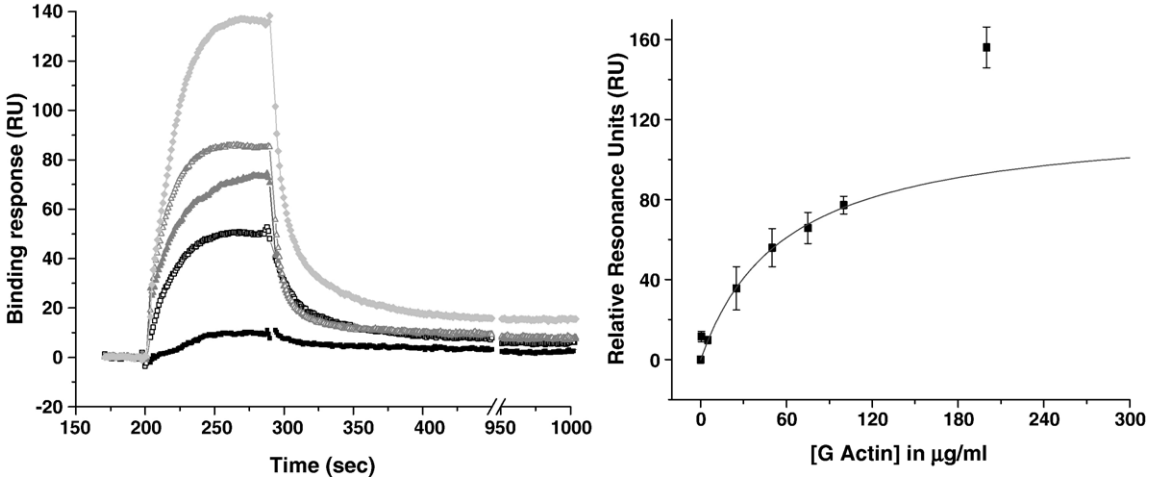

Fig. 1. Dose dependent binding of G-actin to immobilized VDAC. In the left panel, an overlay plot of various sensorgrams resulting from a series of actin concentrations assayed for VDAC binding, 10 (black squares), 25 (black open squares), 75 (grey triangles), 100 (open grey triangles) and 200 (light grey diamonds) μg/ml G-actin (equals 0.2, 0.6, 1.7, 2.3 and 4.7 μM). VDAC immobilization level was ~ 10000 RU. Curves are corrected for bulk effects of both running buffer and negative dilution controls by simple subtraction of the corresponding control sensorgrams. In the right panel, the dose–response curve obtained from the steady-state plateau values (± S.E., $n=9$). Assuming a one-to-one interaction between VDAC and actin, the apparent K_D – derived from the simple hyperbolic fit – is 50 μg/ml (1.2 μM). The SPR signal value obtained at high actin concentration (200 μg/ml actin, 4.7 μM) is shown for illustration propose. It does not fall within the Michaelis–Menten fit and can probably be explained by actin polymerisation (see Discussion for details).

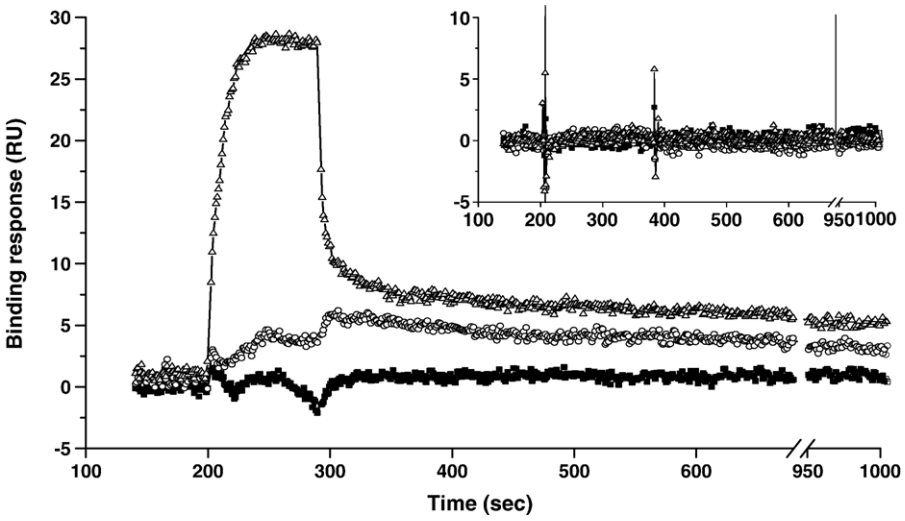

Fig. 3. Specificity of the actin–VDAC interaction. SPR sensorgrams obtained with 3 G-actin concentrations 5 (squares), 50 (circles) and 100 (triangles) μg/ml G-actin (equals 0.1, 1.2, 2.3 μM) binding to VDAC immobilized at ~2000 RU level. The insert shows the absence of response (and of binding) from the identical concentrations of BSA under identical conditions. The data are corrected for bulk effects and dilution controls.

could be seen (identical 1:4 ratio in the upper part of table). This directly links this signal drift to the immobilized VDAC amount. For VDAC binding to actin however, this proportion was slightly higher than can be predicted on the basis of VDAC–VDAC interactions alone. Doubling the coupled molecules on the chip causes a 3-fold increase in slope. This would indicate that roughly 2/3 of the effect could be ascribed to secondary VDAC–VDAC interactions. The remainder is probably the result of more complex interactions within the measurement chamber, including some less specific hydrophobic interactions.

4. Discussion

VDAC is known to interact with a whole set of proteins ranging from cytoskeletal elements, various enzymes and/or apoptotic modulators to viral or bacterial proteins. Recently, the functional interaction between VDAC and actin was reported in planar lipid bilayer [7], although no direct binding was shown. We are reporting here the direct measurements of the actin–VDAC interactions, and of VDAC–VDAC interactions.

Biosensors enable a label-free, real-time investigation of biomolecular interactions. Several instrumentations have been developed (see [22–25] for reviews and comparisons). The Biacore system (Uppsala, Sweden) uses surface plasmon resonance (SPR) and has mainly been applied to determine kinetics and affinity constants [18,26,27]. In all biosensing devices, however, the interpretation of the binding kinetics with first order models requires some caution as deviations from first order reaction are reported due to (i) the invalidity of the model, (ii) rapid interactions leading to mass transfer

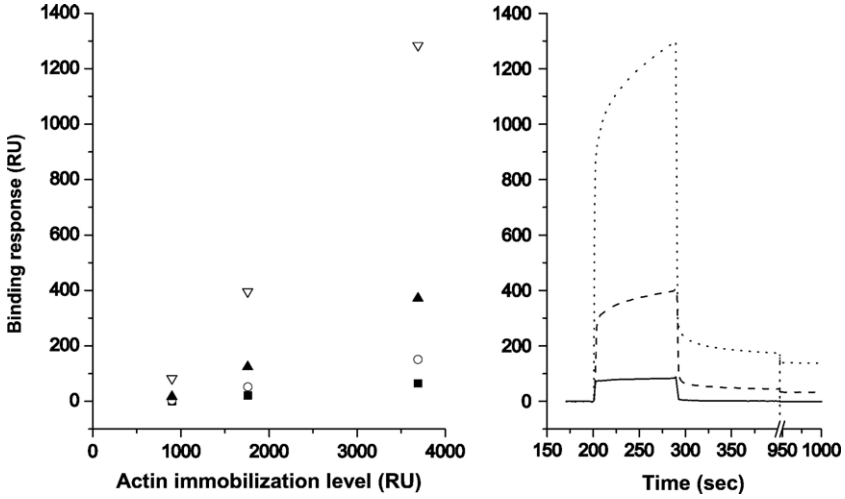

Fig. 4. Binding of VDAC to immobilized actin. In the left panel, the maximal binding responses obtained precisely after a 1.5 min injection for 4 doses of VDAC (50 (squares), 100 (circles), 200 (black triangle) and 500 (open triangle) μg/ml, equals 1.7, 3.3, 6.6, 16.7 μM) at three actin immobilization levels.In the right panel, a given VDAC concentration (500 μg/ml VDAC or 16.7 μM) interacting with actin at three immobilization levels of 900 RU (squares), 1760 RU (circles) and 3690 RU (triangles). Note the drift slope proportional to the immobilization levels.

Table 1
Magnitude of VDAC–VDAC interactions on a sensorchip surface immobilized with VDAC or actin

VDAC on VDAC	VDAC immobilization		Slope	
	RU	Ratio	RU/s	Ratio
	6900	4	0.404	4
	1769	1	0.095	1

VDAC on Actin	Actin immobilization		Slope			
	RU	Ratio	Calculated		Measured	
			RU/s	Ratio	RU/s	Ratio
	6900	4	0.848	4	ND	
	3690	2	0.424	2	0.696	3
	1760	1	(0.212)	1	0.212	1

In the upper panel, the slopes (RU divided by time) of the non saturable binding curves of VDAC on a VDAC-covered sensor chip as measured for 2 chip immobilization levels. A direct proportion can be seen (1:4 ratio) between these parameters. The lower panel shows an identical comparison for VDAC binding on actin. The predicted slopes values (left part) were obtained by assuming that VDAC–VDAC interactions were responsible for the drift. A comparison with the measured drift values shows that the drift is higher. VDAC–VDAC interactions could account for 2/3 of the measured drifts.

limitations [28–30], (iii) ligand site heterogeneity, and (iv) the masking of the potential sites by already bound analyte molecules [31].

In our experiments, pure yeast VDAC1 was captured on the surface of the sensor by amine coupling to measure the interaction with actin in the mobile phase. Ideally for kinetics determination, high flow rates of analyte perfusion (>30 μl/min), low amount of immobilized ligand (around 100's RU), and the use of a reference flow cell are warranted [32]. Although we strictly followed such strategy in early experiments, immobilizations of VDAC as low as 100 RU gave barely readable SPR signals instead of the predicted 143 RU. Using 100 μg/ml actin on 1000 RU immobilized VDAC gave only 4 RU, e.g. We can thus estimate that only 0.3–0.5% of the total prepared surface is likely to be reactive. This is not surprising as VDAC is an integral membrane protein made soluble with 0.1% Triton for the experiments. We captured VDAC directly on the chip without any presenting antibody, thus the coupling procedure allowed it to be bound at random, and therefore the channel, which is devoid of its phospholipid environment, is likely presenting a wide and heterogeneous range of conformations, and it is probable that around 1% of the VDAC sites are only available for eventual 1-to-1 binding. To circumvent this heterogeneity of our ligand sites, we used higher immobilization levels (up to 100× more), and obtained perfectly readable and saturable binding curves.

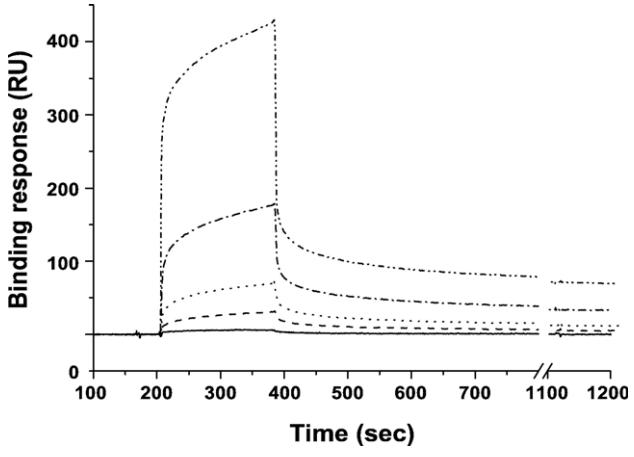

Fig. 5. VDAC–VDAC interactions. Sensorgrams showing VDAC–VDAC binding obtained with 5 VDAC concentrations (5, 25, 50, 100 and 200 μg/ml equals 0.2, 0.8, 1.7, 3.3, 6.6 μM), VDAC immobilization level on the chip at ~6900 RU. Note the drift slopes proportional to the VDAC concentrations used, reflecting second (or higher) order VDAC–VDAC interactions and binding in the measurement chamber.

From these data, an apparent dissociation constant (K_D) of 1.2 μM of actin for VDAC could be derived from the dose–response curve using the plateau values of the binding curves ranging up to 100 μg/ml actin. Such a dissociation constant is comparable with reported affinities for other actin binding proteins like ADF, cofilin [33], Latrunculin A, thymosin β and profilin [34]; all these having a K_D in the micromolar and mainly submicromolar range. Moreover, comparable values are also reported for interactions involving mitochondrial membrane proteins such as components of the mitochondrial import machinery [35,36]. As far as cellular membranes (plasma membranes, mitochondrial membranes and secretory granule membranes) are concerned, the average dissociation constant of another cytoskeletal element, tubulin, is reported to be between 0.15 to 0.3 micromolar. These various values indicate that the apparent K_D of actin for VDAC in this study is comparable to analogous molecular interactions within the cell.

Using actin concentrations above 200 μg/ml (4.7 μM) resulted in values that fell out of the plateau value range and even decreased dramatically at higher concentrations around 400 μg/ml. Although the critical concentration of G-actin was not precisely determined in our conditions, actin polymerisation within the sensor chamber could be responsible for such effect as the resonance signals depend on the refractive index – thus density – near the chip surface. A broad range of critical actin concentrations of 0.1 μM up to 10 μM is reported depending on various factors like its origin [37], the temperature [38], the pH [39], the ATP concentration [40], the presence of Mg^{2+} or Ca^{2+}

[41], the filaments concentration [42], and the interaction with actin binding proteins such as phalloidin [43], latrunculin A [44] or the ADF/cofilin family [33]. Solvent conditions that promote polymerisation include high ionic strength (KCl concentrations >50 mM), neutral or slightly acid pH, high Mg^{2+} (rather than high Ca^{2+}), and elevated temperature.

The cell free system we use contains no magnesium, the major polymerisation factor in a polymerisation buffer. However, $CaCl_2$ was present, Ca^{2+} being less effective for polymerisation [37,41] and the reported concentration of 5 mM $CaCl_2$ is much higher than the maximal 50 μM used in this study. No additional proteins were present in the experimental buffer, nor did it contain F-actin fragments. The experiments were performed at room temperature, with a stabilization phase of 30 min for cold samples. Altogether, these experimental conditions are not per se favourable for a high rate of actin polymerisation. But, because we obtained results respecting the Michaelis–Menten formalism up to 2.3 μM of actin, we assume that polymerisation – if it occurs – starts above 3.5–4.6 μM, a value that falls well within the reported range. With respect to VDAC functional binding, a difference between G-actin and F-actin was seen by Xu et al. as only G-actin was responsible for modulating the voltage dependent gating of VDAC [7]. Thus, it is likely that we are measuring the binding of G-actin to VDAC until some more complex interactions do occur.

As control for the specificity of the direct binding of actin to VDAC, we used the 66 K_D molecule BSA, which is also negatively charged. Binding of BSA to the target should yield higher signals because of its greater mass, but using identical conditions no binding could ever be recorded.

Inverting the roles between ligand and analyte also demonstrated selective binding but the binding kinetics was different. Instead of a plateau in the SPR signal at saturation, a constant drift slope was always present, the magnitude of which depended on the chip's coverage by the bait protein. This could presumably arise because of secondary VDAC–VDAC interactions in the reaction chamber. Since the report that VDAC makes hexagonal clusters in crystalline arrays of the outer membrane of *Neurospora crassa* [19,45], and that it has a preference for the insertion of triplets and multiples of triplets into planar lipid membranes [19], VDAC is known to interact with itself. This property may be used for the auto-directed insertion of VDAC in cell-free membrane systems [15,20], and is shown to be very specific [46]. By looking at VDAC–VDAC binding, we could measure the drift in slope due to VDAC–VDAC interactions. Comparing these slopes to those obtained with VDAC on immobilized actin suggests that the secondary VDAC–VDAC interactions could account for roughly 2/3 of the measured effect. It is worth noting that we use the membrane protein in soluble form; that leaves room for aspecific hydrophobic or surface interactions of the VDAC molecules within the sensor's measuring cell, which could account for the remainder or for a sizeable portion of this drift effect.

The actin–VDAC interaction was previously reported as being restricted to *Neurospora crassa* VDAC and rabbit and porcine muscle actin [7]. However, in that study, a weak and poorly reproducible effect on mammalian VDAC could be found. Here we show a direct binding between *Saccharomyces cerevisiae* VDAC and rabbit muscle actin, hinting a broader spectrum for interspecies interactions. In another study done in our laboratory, the human form of actin was found to be selected by a bait VDAC during phage display screens of a human liver library (M. Zizi, unpublished observations). Function being more restrictive than binding, it is thus highly likely that this interaction is not restricted to VDAC from one species.

The physiological role of this protein–protein interaction is still unclear and can be considered from both partner perspectives. Taking into account the cellular importance and abundance of both proteins, some speculations can be made. As proposed by Xu and co-workers, actin's ability to bind to- and close VDAC may be related to the regulation of energy metabolism. In a metabolically-quiescent cell, a higher free actin concentration could lower mitochondrial function by keeping some of the VDAC channels closed. When a cell becomes more active and uses actin-based systems, free cytosolic G-actin may decrease and thus be displaced from VDAC channels, hence allowing for an increased metabolic flux across and ATP production. Further, a closed VDAC channel – due its inverted ion selectivity – is no longer ATP permeable but becomes permeable to calcium. This alteration in mitochondrial outer membrane permeability could thus influence cellular regulatory processes via Ca^{2+}-dependent proteins. Further, by binding to VDAC, the G-actin could have a direct access to mitochondrial ATP, a situation already reported for hexokinase [47].

Several proteins, binding both VDAC and actin are reported to play a role in apoptotic processes. Gelsolin is an actin-regulatory protein that modulates actin assembly and disassembly. It is reported to prevent apoptosis by inhibiting apoptotic mitochondrial changes via VDAC closure [6]. Actin, on its own right, is suggested as a regulator in apoptosis via interactions with the mitochondria (reviewed in [48]).

The report of the interaction between a channel protein and actin is assuredly not unique. The interaction of the *Neisseria gonorrhoeae* porin – PorIB – with G- and F-actin has been reported, this interaction is impacting the actin polymerisation process and the binding of ATP on the actin molecule [49,50]. Numerous studies have shown binding and/or functional interactions between actin and different ion channels, like ENaC and Ca^{2+}-channels in epithelial cells and neurons [51]. Most of these ion channels interact however with F-actin or short actin filaments.

Regardless of its finality, this interaction between these 2 proteins ought to be further probed as it might impact various cellular functions.

Acknowledgments

This work was supported by grants WB01 and WB03 from Belgium Department of Defense. Jurgen Figys, Griet Steurs and Martin Zizi are supported by the Belgian DoD.

References

[1] M. Colombini, VDAC: the channel at the interface between mitochondria and the cytosol, Mol. Cell. Biochem. 256–257 (2004) 107–115.

[2] E.H. Cheng, T.V. Sheiko, J.K. Fisher, W.J. Craigen, S.J. Korsmeyer, VDAC2 inhibits BAK activation and mitochondrial apoptosis, Science 301 (2003) 513–517.

[3] T.K. Rostovtseva, W. Tan, M. Colombini, On the role of VDAC in apoptosis: fact and fiction, J. Bioenerg. Biomembr. 37 (2005) 129–142.

[4] M. Linden, G. Karlsson, Identification of porin as a binding site for MAP2, Biochem. Biophys. Res. Commun. 21 (1996) 833–836.

[5] C. Schwarzer, S. Barnikol-Watanabe, F.P. Thinnes, N. Hilschmann, Voltage-dependent anion-selective channel (VDAC) interacts with the dynein light chain Tctex1 and the heat-shock protein PBP74, Int. J. Biochem. Cell Biol. 34 (2002) 1059–1070.

[6] H. Kusano, S. Shimizu, R.C. Koya, H. Fujita, S. Kamada, N. Kuzumaki, Y. Tsujimoto, Human gelsolin prevents apoptosis by inhibiting apoptotic mitochondrial changes via closing VDAC, Oncogene 19 (2000) 4807–4814.

[7] X. Xu, J.G. Forbes, M. Colombini, Actin modulates the gating of *Neurospora crassa* VDAC, J. Membr. Biol. 180 (2001) 73–81.

[8] C.G. dos Remedios, D. Chhabra, M. Kekic, I.V. Dedova, M. Tsubakihara, D.A. Berry, N.J. Nosworthy, Actin binding proteins: regulation of cytoskeletal microfilaments, Physiol. Rev. 83 (2003) 433–473.

[9] G.G. Borisy, T.M. Svitkina, Actin machinery: pushing the envelope, Curr. Opin. Cell Biol. 12 (2000) 104–112.

[10] V.R. Simon, T.C. Swayne, L.A. Pon, Actin-dependent mitochondrial motility in mitotic yeast and cell-free systems: identification of a motor activity on the mitochondrial surface, J. Cell Biol. 130 (1995) 345–354.

[11] I. Boldogh, N. Vojtov, S. Karmon, L.A. Pon, Interaction between mitochondria and the actin cytoskeleton in budding yeast requires two integral mitochondrial outer membrane proteins, Mmm1p and Mdm10p, J. Cell Biol. 141 (1998) 1371–1381.

[12] R.L. Morris, P.J. Hollenbeck, Axonal transport of mitochondria along microtubules and F-actin in living vertebrate neurons, J. Cell Biol. 131 (1995) 1315–1326.

[13] I. Roman, J. Figys, G. Steurs, M. Zizi, A systematic search for physiologically relevant ligands of the mitochondrial membrane protein VDAC, Biophys. J. 86 (Suppl. 1) (2004) 358 (Part 2-2).

[14] X. Xu, M. Colombini, Autodirected insertion: preinserted VDAC channels greatly shorten the delay to the insertion of new channels, Biophys. J. 72 (1997) 2129–2136.

[15] M. Zizi, L. Thomas, E. Blachly-Dyson, M. Forte, M. Colombini, Oriented channel insertion reveals the motion of a transmembrane beta strand during voltage gating of VDAC, J. Membr. Biol. 144 (1995) 121–129.

[16] V. De Pinto, G. Prezioso, F. Palmieri, A simple and rapid method for the purification of the mitochondrial porin from mammalian tissues, Biochim. Biophys. Acta 905 (1987) 499–502.

[17] F. Palmieri, V. De Pinto, Purification and properties of the voltage-dependent anion channel of the outer mitochondrial membrane, J. Bioenerg. Biomembr. 21 (1989) 417–425.

[18] D.G. Myszka, Kinetic analysis of macromolecular interactions using surface plasmon resonance biosensors, Curr. Opin. Biotechnol. 8 (1997) 50–57.

[19] C.A. Mannella, M. Colombini, J. Frank, Structural and functional evidence for multiple channel complexes in the outer membrane of *Neurospora crassa* mitochondria, Proc. Natl. Acad. Sci. U. S. A. 80 (1983) 2243–2247.

[20] X. Xu, M. Colombini, Self-catalyzed insertion of proteins into phospholipid membranes, J. Biol. Chem. 271 (1996) 23675–23682.

[21] R. Zalk, A. Israelson, E.S. Garty, H. Azoulay-Zohar, Oligomeric states of the voltage-dependent anion channel and cytochrome *c* release from mitochondria, Biochem. J. 386 (2005) 73–83.

[22] M.A. Cooper, Label-free screening of bio-molecular interactions, Anal. Bioanal. Chem. 377 (2003) 834–842.

[23] C. Hahnefeld, S. Drewianka, F.W. Herberg, Determination of kinetic data using surface plasmon resonance biosensors, Methods Mol. Med. 94 (2004) 299–320.

[24] R.J. Leatherbarrow, P.R. Edwards, Analysis of molecular recognition using optical biosensors, Curr. Opin. Chem. Biol. 3 (1999) 544–547.

[25] R.L. Rich, D.G. Myszka, Survey of the year 2003 commercial optical biosensor literature, J. Mol. Recognit. 18 (2005) 1–39.

[26] M. Malmqvist, R. Karlsson, Biomolecular interaction analysis: affinity biosensor technologies for functional analysis of proteins, Curr. Opin. Chem. Biol. 1 (1997) 378–383.

[27] P. Schuck, Reliable determination of binding affinity and kinetics using surface plasmon resonance biosensors, Curr. Opin. Biotechnol. 8 (1997) 498–502.

[28] R.W. Glaser, Antigen–antibody binding and mass transport by convection and diffusion to a surface: a two-dimensional computer model of binding and dissociation kinetics, Anal. Biochem. 213 (1993) 152–161.

[29] D.R. Hall, J.R. Cann, D.J. Winzor, Demonstration of an upper limit to the range of association rate constants amenable to study by biosensor technology based on surface plasmon resonance, Anal. Biochem. 235 (1996) 175–184.

[30] D.G. Myszka, X. He, M. Dembo, T.A. Morton, B. Goldstein, Extending the range of rate constants available from BIACORE: interpreting mass transport-influenced binding data, Biophys. J. 75 (1998) 583–594.

[31] D.J. O'Shannessy, D.J. Winzor, Interpretation of deviations from pseudo-first-order kinetic behavior in the characterization of ligand binding by biosensor technology, Anal. Biochem. 236 (1996) 275–283.

[32] D.G. Myszka, T.A. Morton, M.L. Doyle, I.M. Chaiken, Kinetic analysis of a protein antigen–antibody interaction limited by mass transport on an optical biosensor, Biophys. Chem. 64 (1997) 127–137.

[33] S. Yeoh, B. Pope, H.G. Mannherz, A. Weeds, Determining the differences in actin binding by human ADF and cofilin, J. Mol. Biol. 315 (2002) 911–925.

[34] E.G. Yarmola, T. Somasundaram, T.A. Boring, I. Spector, M.R. Bubb, Actin–latrunculin A structure and function. Differential modulation of actin-binding protein function by latrunculin A, J. Biol. Chem. 275 (2000) 28120–28127.

[35] M. Esaki, T. Kanamori, S. Nishikawa, I. Shin, P.G. Schultz, T. Endo, Tom40 protein import channel binds to non-native proteins and prevents their aggregation, Nat. Struct. Biol. 10 (2003) 988–994.

[36] E. Schleiff, J.L. Turnbull, Functional and structural properties of the mitochondrial outer membrane receptor Tom20, Biochemistry 37 (1998) 13043–13051.

[37] D.J. Gordon, Y.Z. Yang, E.D. Korn, Polymerization of Acanthamoeba actin. Kinetics, thermodynamics, and co-polymerization with muscle actin, J. Biol. Chem. 251 (1976) 7474–7479.

[38] C.T. Zimmerle, C. Frieden, Effect of temperature on the mechanism of actin polymerization, Biochemistry 25 (1986) 6432–6438.

[39] C.T. Zimmerle, C. Frieden, Effect of pH on the mechanism of actin polymerization, Biochemistry 27 (1988) 7766–7772.

[40] B.M. Fung, E. Eyob, The effect of ATP concentration on the rate of actin polymerization, Arch. Biochem. Biophys. 220 (1983) 370–378.

[41] D.J. Gordon, J.L. Boyer, E.D. Korn, Comparative biochemistry of non-muscle actins, J. Biol. Chem. 252 (1977) 8300–8309.

[42] D. Pantaloni, M.F. Carlier, M. Coue, A.A. Lal, S.L. Brenner, The critical concentration of actin in the presence of ATP increases with the number concentration of filaments and approaches the critical concentration of actin.ADP, J. Biol. Chem. 259 (1984) 6274–6283.

[43] P. Dancker, I. Low, W. Hasselbach, T. Wieland, Interaction of actin with phalloidin: polymerization and stabilization of F-actin, Biochim. Biophys. Acta 400 (1975) 407–414.

[44] W.M. Morton, K.R. Ayscough, P.J. McLaughlin, Latrunculin alters the actin–monomer subunit interface to prevent polymerization, Nat. Cell Biol. 2 (2000) 376–378.

[45] C.A. Mannella, Mitochondrial outer membrane channel (VDAC, porin) two-dimensional crystals from Neurospora, Methods Enzymol. 125 (1986) 595–610.

[46] X.X. Li, M. Colombini, Catalyzed insertion of proteins into phospholipid membranes: specificity of the process, Biophys. J. 83 (2002) 2550–2559.

[47] V. Adams, L. Griffin, J. Towbin, B. Gelb, K. Worley, E.R. McCabe, Porin

interaction with hexokinase and glycerol kinase: metabolic microcompartmentation at the outer mitochondrial membrane, Biochem. Med. Metabol. Biol. 45 (1991) 271–291.
[48] C.W. Gourlay, L.N. Carpp, P. Timpson, S.J. Winder, K.R. Ayscough, A role for the actin cytoskeleton in cell death and aging in yeast, J. Cell Biol. 164 (2004) 803–809.
[49] K.K. Wen, P.C. Giardina, M.S. Blake, J. Edwards, M.A. Apicella, P.A. Rubenstein, Interaction of the gonococcal porin P.IB with G- and F-actin, Biochemistry 39 (2000) 8638–8647.
[50] K.K. Wen, M.S. Blake, P.A. Rubenstein, *Neisseria gonorrhoeae* porin, P. IB, causes release of ATP from yeast actin, J. Muscle Res. Cell Motil. 25 (2004) 343–350.
[51] H.F. Cantiello, Role of actin filament organization in cell volume and ion channel regulation, J. Exp. Zool. 279 (1997) 425–435.